ACS APPLIED MATERIALS & INTERFACES

Research Article

www.acsami.org

Sensitivity of Diamond-Capped Impedance Transducer to Tröger's Base Derivative

Stepan Stehlik,[†,*] Tibor Izak,[†] Alexander Kromka,[†] Bohumil Dolenský,[‡] Martin Havlík,[‡] and Bohuslav Rezek[†]

[†]Institute of Physics, Academy of Sciences of the Czech Republic, v.v.i., Cukrovarnická 10, 162 00, Prague 6, Czech Republic

[‡]Department of Analytical Chemistry, Institute of Chemical Technology Prague, Technická 5, 166 28, Prague 6, Czech Republic

Supporting Information

ABSTRACT: Sensitivity of an intrinsic nanocrystalline diamond (NCD) layer to naphthalene Tröger's base derivative decorated with pyrrole groups (TBPyr) was characterized by impedance spectroscopy. The transducer was made of Au interdigitated electrodes (IDE) with 50 μm spacing on alumina substrate which were capped with the NCD layer. The NCD-capped transducer with H-termination was able to electrically distinguish TBPyr molecules (the change of surface resistance within 30−60 kΩ) adsorbed from methanol in concentrations of 0.04 mg/mL to 40 mg/mL. An exponential decay of the surface resistance with time was observed and attributed to the readsorption of air moisture after methanol evaporation. After surface oxidation the NCD cap layer did not show any leakage due to NCD grain boundaries. We analyzed electronic transport in the transducer and propose a model for the sensing mechanism based on surface ion replacement.

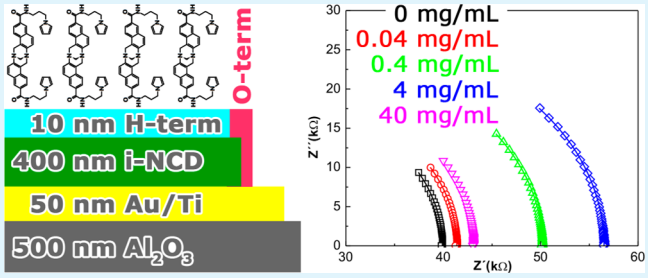

KEYWORDS: *Tröger's base derivative, nanocrystalline diamond, chemical sensor, impedance spectroscopy, surface conductivity*

INTRODUCTION

Tröger's base (TB) has attracted a lot of attention since its first synthesis by Julius Tröger in 1887[1] (Figure 1). The structure of

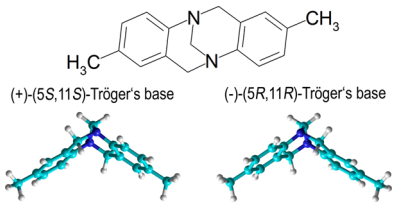

Figure 1. Structure of TB molecule.

this molecule is often used to demonstrate the capability of nitrogen atom to act as a chiral center. Considerable interest, especially in the functionalized analogues of Tröger's base, has started in the second half of 1980s since this V-shaped molecule offers applications as a unique building block for unusual molecular designs. Various functional groups were bonded to the opposite ends of the V-shaped molecule of TB to create synthetic receptors for the recognition of adenine derivatives,[2,3] dicarboxylic acids,[4] DNA[5] interactions etc. If combined with large π-conjugated aryl substituted fluorene, anthracene, or pyridinium salts TB can serve as organic light-emitting material.[6] Generally, π-conjugated systems can mediate the electrical response to a transducer device which is crucial in many application areas, such as electronics, chemistry, or medicine. The chemistry and various applications of Tröger's base derivatives are regularly reviewed.[7−9]

However, electrical detection of TB properties has not been accomplished so far. In that context, diamond offers a great application potential as an electrically active interface to TB with a possibility to tailor its structural, chemical, and electronic properties. Electronic properties of CVD (Chemical Vapor Deposition) diamond can be tuned from an insulator to a semiconductor. Taking into account its hardness, chemical stability and biocompatibility, diamond is considered a promising material for various sensors and biosensors. Recently, a new generation of gas sensors based on a change of surface conductivity of H-terminated intrinsic diamond upon the gas adsorption has been introduced with different sensor designs.[10,11] Our group has demonstrated that interdigitated electrodes (IDE) capped with nanostructured H-NCD are highly sensitive and selective to phosgene gas that dissolves in the surface adsorbate layer and increases surface conductivity of H-terminated diamond.[12,13] Such sensors are, in general, structurally, chemically, and electronically complex systems, and it is not straightforward to distinguish particular contributions of their overall electric response. Because the NCD is a polycrystalline material, it is generally accepted that three conductivity contributions can be distinguished in an

Received: April 3, 2012
Accepted: July 6, 2012
Published: July 6, 2012

intrinsic NCD layer. Those are the grain interior conductivity, grain boundary (GB) conductivity and grain surface (GS) conductivity.[14−17] However, the above-mentioned studies used a sandwich arrangement of the electrodes with the NCD layer as the probed material in between. This arrangement can extract important electrical parameters of a material under study but cannot be used to investigate the electric response of a surface nor be used as a chemical sensor.

Impedance spectroscopy is recognized as a useful and powerful technique for such tasks. A common approach of using gold interdigitated electrodes covered by a sensing material becomes surprisingly efficient if an intrinsic, resistive NCD layer is used as the sensing material. Such transducers worked for gas detection,[13] albeit without explaining details of the electronic transport.

By using the impedance spectroscopy we demonstrate here that the NCD capped IDE transducer is able to electrically distinguish various concentrations of the naphthalene TB derivative having pyrrole moieties (TBPyr) adsorbed from dispersion in methanol. We used TBPyr as a potential molecular receptor. Another advantage is that it can be electrochemically grafted to the diamond surface[18,19] through the pyrrole moieties. We show that surface H-termination is fundamental for the transducer performance as a sensor. We present analysis of electronic transport properties in the NCD-capped transducer and propose a model of the sensing mechanism.

EXPERIMENTAL SECTION

TBPyr derivative was prepared from TBOMe according to Scheme 1 via the following procedures. Diester TBOMe (2.0 g, 4.6 mmol)[20] was

Scheme 1. Preparation of TBPyr and Arbitrary Numbering

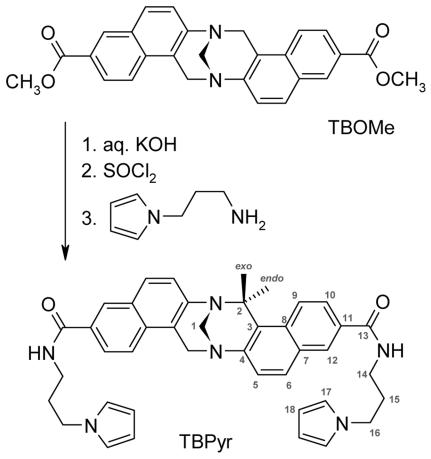

treated with 3 M aq. KOH (100 mL) in ethanol (100 mL) at 75 °C overnight. The reaction mixture was neutralized by acetic acid. The precipitated solid was filtered off, washed with water, methanol and dried in vacuo to obtain 1.8 g (97%) of diacid. ^{1}H NMR (300 MHz, DMSO-d_6): δ 12.99 (2H, bs), 8.44 (2H, d, 1.7), 7.94 (2H, dd, 8.8, 1.7), 7.90 (2H, d, 8.8), 7.83 (2H, d, 8.8), 7.45 (2H, d, 8.8), 5.00 (2H, d, 17.0), 4.79 (2H, d, 17.0), 4.47 (2H, s). ^{13}C APT NMR (75 MHz, DMSO-d_6): δ 167.38 (C), 147.58 (C), 133.12 (C), 130.82 (CH), 129.36 (C), 128.69 (CH), 126.61 (C), 125.85 (CH), 125.50 (CH), 121.85 (CH), 121.45 (C), 65.75 (CH_2), 55.13 (CH_2). HRMS (ESI$^-$) for $C_{25}H_{17}N_2O_4$ [M-H]$^-$ calcd 409.11828, found 409.11914.

Diacid (200 mg, 0.5 mmol) was treated with $SOCl_2$ (4 mL) at 80 °C for 3 h. The resulting solution was evaporated in vacuo to dryness. The residual solid was dissolved in tetrahydrofurane (10 mL), *N*-(3-aminopropyl)pyrrole (133 mg, 1.1 mmol) and Et_3N (168 mg, 1.2 mmol) was added. The mixture was stirred overnight at room temperature. The reaction mixture was evaporated to dryness in vacuo. The residue was separated by column chromatography (dichloromethane/methanol 95:5) to obtain 267 mg (88%) of diamide TBPyr. ^{1}H NMR (DMSO-d_6): δ 8.57 (2H, t, 5.5, NH), 8.31 (2H, d, 1.7, H12), 7.91 (2H, dd, 8.8, 1.7, H10), 7.81 (2H, d, 8.8, H9), 7.81 (2H, d, 8.8, H6), 7.46 (2H, d, 8.8, H5), 6.78 (4H, t, 2.1, H17), 5.97 (4H, t, 2.1, H18), 4.97 (2H, d, 17.0, H2^{exo}), 4.78 (2H, d, 17.0, H2^{endo}), 4.46 (2H, s, H1), 3.93 (4H, t, 6.9, H16), 3.24 (4H, q, H14), 1.95 (4H, qn, H15). ^{13}C APT NMR (75 MHz, DMSO-d_6): δ 166.12 (C13), 146.90 (C4), 132.23 (C8), 130.41 (C11), 129.36 (C7), 128.29 (C6 or C10), 127.84 (C12), 125.47 (C5 or C9), 124.78 (C6 or C10), 121.62 (C5 or C9), 121.45 (C3), 120.59 (C17), 107.53 (C18), 65.88 (C1), 55.17 (C2), 46.47 (C16), 36.93 (C14), 31.24 (C15). HRMS (ESI$^+$) for $C_{39}H_{38}N_6O_2Na$ [M+Na]$^+$ calcd 645.29485, found 645.29447.

For the electrical transducer, the Ti/Au electrodes (Ti/Au = 30/50 nm) were deposited on the polycrystalline Al_2O_3 substrates by thermal evaporation method in vacuum. The IDE structure was fabricated by means of standard UV-lithography and lift-off technique. The gap between IDE was 50 μm. Then, the substrates were seeded by an aqueous dispersion of detonation diamond powder (average grains size 5 nm) in an ultrasonic bath for 40 min.[21] The NCD layer was deposited by microwave plasma chemical vapor deposition process in Aixtron P6 reactor.[22] The deposition was performed using the following parameters: microwave power 1000 W, total gas pressure 30 mbar, 1% of methane diluted in hydrogen, temperature 400 °C, and deposition time 5 h. The thickness of the deposited NCD films was about 400 nm as determined optically from a smooth reference sample.

To check the quality of the NCD layer both on Au contacts and ceramic substrate the SEM images were taken by MIRA3 Tescan microscope. The coverage of the transducer after application of TBPyr suspensions was also investigated by SEM.

For the impedance measurements of O-terminated surface, the diamond surface was oxidized by rf oxygen plasma process (300 W, 3 min). For the impedance measurements of H-terminated surface, a stripe of oxidized surface was covered by an SU-8 photoresist at the border to the contacts (to prevent shunts) and the rest of the NCD surface was H-terminated in hydrogen microwave plasma (450 °C, 40 mbar, 2900 W, 10 min). Finally the SU-8 photoresist was removed by acetone. Measurements of water contact angle showed clear difference between wetting of H- and O-terminated NCD surfaces. The contact angles were 91° and 6° for H-terminated and O-terminated surface, respectively. Control measurement on the films deposited under the same conditions on smooth glass substrate showed contact angle approximately 90° for H-terminated surface. Figure 2 shows the scheme of the transducer in top and cross-sectional view with an idealized visualization of TBPyr molecules adsorbed onto the surface.

Impedance spectra were measured using a HIOKI 3532−50 LCR analyzer in a frequency range of 100 kHz to 10 Hz at room temperature. The amplitude of the AC voltage was 0.5 V. The impedance response of the transducer to pure methanol was checked prior to measurements with TBPyr suspensions.

TBPyr suspensions in methanol were prepared by sequential dilution of the most concentrated suspension IV (40 mg/mL), providing concentrations III (4 mg/mL), II (0.4 mg/mL) and I (0.04 mg/mL). The suspensions III and IV were milky and sedimentation occurred within few minutes. For testing the impedance response of the transducer, the suspension was ultrasonicated for 2 min and 1 μL of the suspension was applied onto the transducer using a micropipet. Methanol was evaporated spontaneously in few seconds and the impedance spectrum was measured after 5, 10, 20, 40, and 60 min. The suspensions were measured from the lowest concentrated suspension I to the most concentrated suspension IV. Once the measurement was finished the transducer was rinsed and ultrasonicated for 2 min in pure methanol and then blown dried and reused for a next set of measurements. This procedure led to reproducible recovery of the sensor condition.

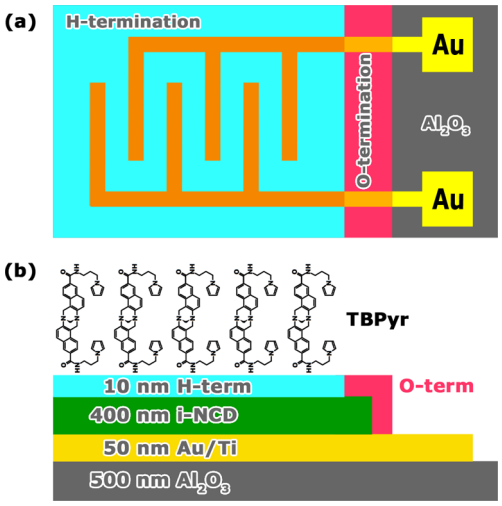

Figure 2. Schematic drawing of diamond-capped IDE transducer device. (a) Top view and (b) cross-sectional view with an idealized visualization of adsorbed TBPyr molecules on the H-terminated diamond surface.

RESULTS

Results of SEM characterizations are shown in Figure 3. Figure 3a shows the initial Al_2O_3 ceramic surface prior to the NCD

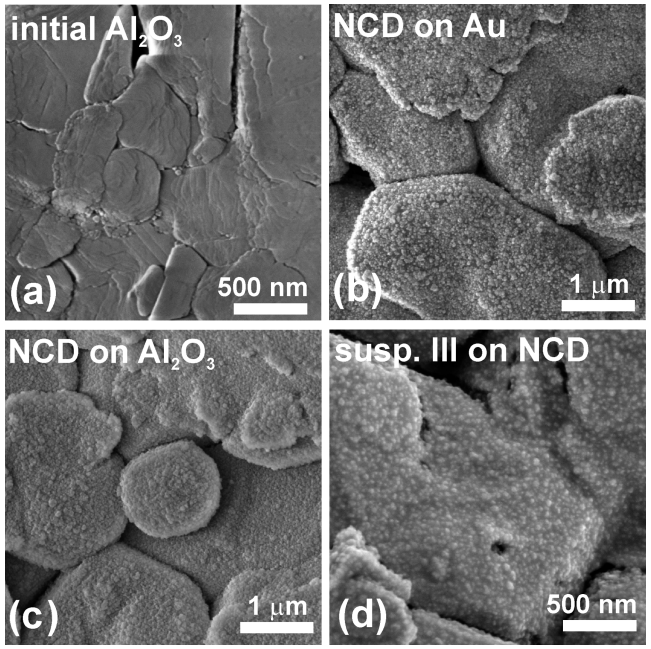

Figure 3. SEM images of (a) initial Al_2O_3 substrate, (b) NCD layer as grown on Au electrodes, and (c) on Al_2O_3 substrate. (d) The coverage of the NCD surface by TBPyr molecules adsorbed from suspension III.

growth. Relatively smooth grains of the ceramics with various sizes are visible on the surface. After the NCD growth the grains are fully covered with a thin diamond layer both on Au contacts and on the Al_2O_3 substrate (Figure 3b, c). As an example the coverage of the NCD layer by TBPyr molecules as adsorbed from the suspension III is shown in Figure 3d. It is visible that the layer of the molecules does not fully cover the NCD surface but rather fills the space between the tops of diamond nanocrystals. The rest of SEM images (not presented here) showed almost no detectable coverage of suspensions I and II and very dense, continuous layer formed by the most concentrated suspension IV.

The impedance spectra were fitted by $R_1(CR_2)$ equivalent circuit which produced reliable physical parameters. We have found that while the value R_1 remained relatively stable for all the measurement 3 ± 1 kΩ, the resistance R_2 of the H-terminated transducer strongly varied depending on the conditions on the transducer surface as shown further on.

Figure 4 shows the impedance spectra as a function of time after application of pure methanol droplet onto the H-

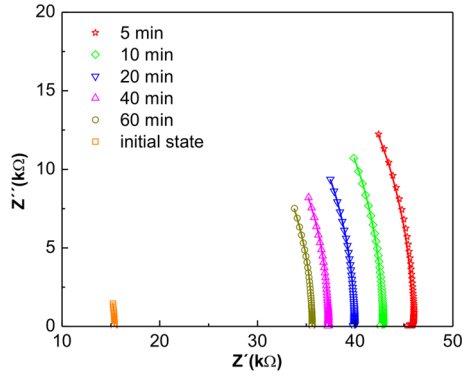

Figure 4. Time dependence of impedance spectra of the H-terminated transducer after a droplet of methanol is applied onto its surface. The symbols corresponding to particular measurement times are given in the legend of the graph. The lines correspond to the equivalent circuit fits.

terminated NCD surface. The values of R_2 measured 5 min after application of methanol droplet were approximately three times higher than the total resistance in the initial state and gradually decreased. This effect seems to be general as similar behavior was observed also after application of TBPyr suspensions with various concentrations.

This is easily recognizable from the Figure 5 where the obtained values of total resistance R_2 as a function of time were fitted by an exponential decay function of the first order. The time constant varied between 17 and 25 min without a clear

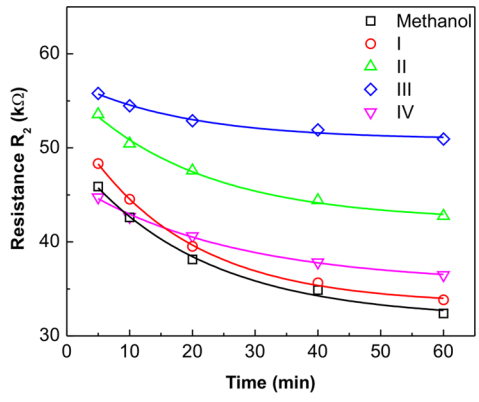

Figure 5. Dependence of resistance R_2 on time for TBPyr suspensions and pure methanol. The lines correspond to fits of exponential decay of the first order. Particular suspensions are denoted as follows: black squares, methanol; red circles, suspension I (0.04 mg/mL); green triangles, suspension II (0.4 mg/mL); blue diamonds, suspension III (4 mg/mL); and upturned purple triangles, suspension IV (40 mg/mL).

dx.doi.org/10.1021/am3005829 | ACS Appl. Mater. Interfaces 2012, 4, 3860−3865

trend as a function of suspension concentration. On the other hand, and more importantly, the resistance R_2 depends on the TBPyr concentration. Full impedance spectra measured 20 min after TBPyr application (chosen as case example) are shown in Figure 6 (a). They confirm this effect in the full spectral range.

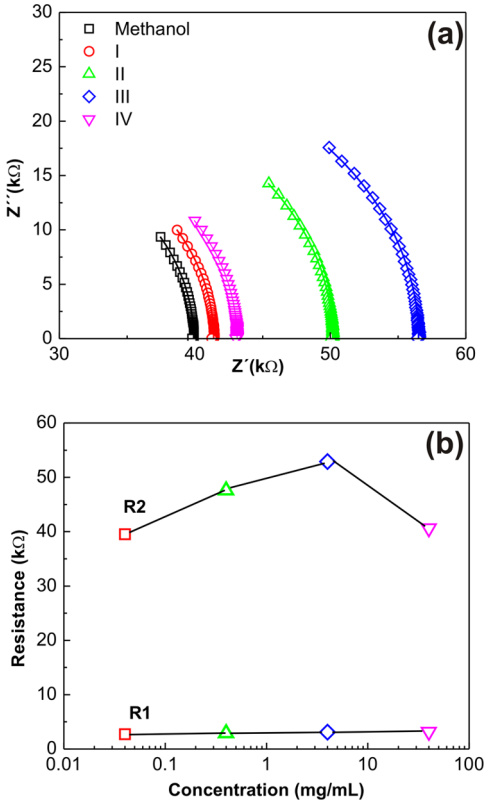

Figure 6. (a) Impedance spectra as measured after 20 min. The lines in the impedance spectra correspond to $R_1(CR_2)$ equivalent circuit fits. (b) Values of resistances R_1 and R_2 as function of concentration obtained from the fits after 20 min. Particular suspensions are denoted as follows: black squares, methanol; red circles, suspension I (0.04 mg/mL); green triangles, suspension II (0.4 mg/mL); blue diamonds, suspension III (4 mg/mL); and upturned purple triangles, suspension IV (40 mg/mL).

We can also see that the simple $R_1(CR_2)$ model fits the spectra well. We observed an increase of the resistance R_2 from 40 kΩ to 57 kΩ with increasing concentration of TBPyr molecules for suspensions I to III. The most concentrated suspension IV did not follow this trend and resistance has decreased again to about 42 kΩ. The values of resistances R_1 and R_2 as obtained from the fits after 20 min are plotted as a function of TBPyr suspension concentration in Figure 6 (b).

The O-terminated transducer was investigated by impedance spectroscopy in the same manner as was the H-terminated. The values of R_1 were 3 ± 1 kΩ such as in the case of H-terminated transducer. The values of R_2 are on the order of 1×10^8 Ω for all the measurements. However, the impedance spectra of the O-terminated transducer lacked reliable low frequency data, so it was impossible to fit the spectra with high-enough accuracy to resolve the influence of TBPyr adsorption.

DISCUSSION

Quality of the diamond layer, especially its uniformity (pinhole-free), is crucial if one wants to obtain reliable data from the impedance sensor. It is known that NCD layers do not easily grow on Au and on alumina because these materials do not form carbide connective layer and a thicker NCD layer may delaminate from the surface.[23] From Figure 3, it is obvious that the fabricated impedance transducer is uniformly coated with a thin NCD layer that fully covers both Au contacts and ceramic substrate. We did not observe any indication of delamination even after repeated use. This is probably because of a good coating uniformity, reduced deposition temperature (400 °C), and relatively low thickness (~400 nm).

To understand the sensing mechanism of H-NCD sample we must first assign the resistances R_1 and R_2 to their corresponding physical mechanisms. Since we have found out that the resistance R_1 did not depend on the surface termination (the same values for H- and O-terminated NCD) and was not influenced by any surface treatment we attribute it to a transverse resistance of the NCD layer. The resistance R_2 then corresponds to a longitudinal surface resistance. The R_1 value of 3 kΩ seems low for the intrinsic NCD, but this is due to the small layer thickness. Recalculated to resistivity it corresponds to 2×10^6 Ωcm which is a reasonable value when we consider nanocrystalline character of the film with grain boundaries. Note also, that this transverse resistance is an order of magnitude smaller than longitudinal resistance along the film (corresponding to $\sim 6 \times 10^7$ Ωcm as obtained from $R_2 \approx 1 \times 10^8$ Ω on O-NCD) because of the anisotropy in the NCD film microstructure.[24]

On H-NCD the longitudinal resistance R_2 in the range of ~10 kΩ reflects existence of the so-called surface conductive layer on H-terminated surface and surface-related effects are responsible for its changes. The value of R_2 ~10 kΩ corresponds to sheet resistivity of $\sim 1.5 \times 10^7$ Ω/sq. This value is in agreement with typical sheet resistivity of H-NCD as observed by Hall-effect measurements.[25] The concentration of carriers obtained by these Hall effect measurements was on the order of 10^{13} cm^{-2} as in the monocrystalline diamond. The electronic transport in H-NCD is thus limited by hopping across the grain boundaries that reduces carrier mobility (down to about 1 $cm^2/(V\ s)$). Yet the grain boundaries are not detrimental for the transducer function. As concluded by the studies of proteins by solution-gated field-effect transistors made of H-NCD,[26,27] it is the H-terminated surface that determines the function of H-NCD as an electronic interface to the molecules. High value of resistance $R_2 \approx 1 \times 10^8$ Ω in the case of O-NCD cap layer confirms that the IDE is not shortcut by graphitic phase at the NCD grain boundaries and that the surface conductivity plays a crucial role in the function of the transducer.

It has been shown in Figure 4 that after the methanol application the surface resistance increases at first and then decreases with time. Similar decay was observed in the case of TBPyr dispersions in methanol. As the methanol quickly evaporates it is reasonable to suppose that the moisture adsorbed on the surface from air is effectively removed by this process (well-known drying effect of alcohols). Because the surface conductivity of diamond relies on the presence of an adsorbed water film on the hydrophobic H-terminated diamond surface[28−30] (though its molecular arrangement is different from the O-terminated surface[31]), the surface resistance increases at first. The subsequent exponential decay of the surface resistance, similar in all cases, is most likely caused by the readsorption of air moisture until a new balance is reached.

The electrical sensitivity of H-NCD surface to various concentrations of TBPyr proves that the H-NCD surface is electrically active and an electronic interaction between surface and its vicinity occurs. This could be an electrostatic field effect or some kind of a charge transfer. Wang[10] proposed a model based on electron transfer from diamond to an oxidizing gas adsorbate layer (e.g., NO_2) which can lead to an increase in the surface conductivity of the H-NCD layer. On the other hand, when electrons were transferred from a reducing gas adsorbates (e.g., NH_3) to diamond, the surface conductivity decreased. Helwig et al.[11] proposed a more detailed model and explained the sensitivity of H-NCD to NO_2 and NH_3 gases on the basis of surface transfer doping model, i.e. the local changes of pH in the thin water layer present on the H-NCD surface are responsible for these effects. The exposure of H-NCD surface to NO_2 leads to an increased concentration of H_3O^+ ions which could act as acceptors for electrons coming from the valence bands of H-NCD and thus increasing the concentration of holes in the H-NCD surface layer. Davydova et al. explained in the same manner the increase of the surface conductivity of H-NCD during exposure to phosgene.[21] On the other hand the exposure to NH_3 led to a decrease in H_3O^+ concentration and so the decrease of surface conductivity occurred.

In light of the above models, we identify one possible mechanism that may be responsible for the increase of the surface resistance after adsorption of TBPyr molecules. These molecules have basic character and, although practically water insoluble, they can in principle become protonated to some extent and thus decrease the concentration of H_3O^+ ions in the surface vicinity. This may result in the observed decrease in surface conductivity.

However, when we consider that the TBPyr molecules are dispersed but not actually dissolved in the suspension and we observed formation of solid adsorbed film by SEM, we can conclude that the mechanism of its action is probably different to that of gases. In addition, there is no special reason why the TBPyr should become significantly protonated and charged in a suspension or on the surface. Thus pH and electrostatic field effects of molecules on the surface conductivity are probably negligible.

Another possible mechanism may be similar as reported by Rezek et al.[26] where the decrease of surface conductivity of H-NCD was attributed to a replacement of surface ions by adsorbed proteins. In principle, this mechanism can be considered as a change of local pH, and hence to be in line with the concept of transfer doping model. On the basis of the considerations above, this mechanism is most likely to be valid. Nevertheless, to what degree this "mechanical" surface ion replacement by TBPyr contributes to the transducer sensitivity, to what degree the TBPyr becomes protonated because of chemical reaction in the surface vicinity, and to what degree TBPyr becomes charged and influences the surface conductivity by electrostatic field effect, still remains to be elucidated.

Deviation of the most concentrated suspension IV from the observed trend is also noteworthy. The sudden decrease of resistance cannot be caused by charge transfer to H-NCD as this should be a uniform trend also at lower concentrations. Another possibility is that the dense TBPyr layer becomes conductive itself and "shunts" the transducer. However, impedance measurement on the Au IDE structure (without NCD layer) after application of the suspension IV showed a very large resistance of the adsorbed TBPyr layer. Same observation was done on the O-NCD capped transducer. Thus, the dense TBPyr layer itself is not conductive enough to explain the decrease of resistance. Still, there is a remote possibility that the configuration of TBPyr molecular layers on Au, alumina, and O-NCD may be different than on H-NCD, in similarity to proteins adsorbed on diamonds.[32]

CONCLUSION

We have successfully fabricated and demonstrated functionality of H-NCD capped IDE as an electrical transducer sensitive to TBPyr molecules. The grain boundaries were not detrimental for its function. This demonstrates the feasibility of coating diverse sensor structures by NCD that can provide improved or completely new specific functions. Impedance spectroscopy resolved that the transducer response is given by a change in the longitudinal surface conductivity while transverse resistance of NCD cap layer remains constant under all conditions and surface terminations. The H-terminated transducer is able to distinguish various concentrations of TBPyr suspensions. On the other hand, the O-terminated sample did not provide reliable low frequency data to resolve this effect. We proposed a model where TBPyr molecules replace ions in the surface vicinity, in correlation with a similar model for protein adsorption on diamond. Further work is still needed to clarify the details of the mechanism though. Nevertheless, we believe that the results already show the way for electronic sensing of TBPyr molecular receptors using specific properties of nanocrystalline diamond.

ASSOCIATED CONTENT

Supporting Information

NMR spectra of diacid intermediate and TBPyr (PDF). This material is available free of charge via the Internet at http://pubs.acs.org

AUTHOR INFORMATION

Corresponding Author

*E-mail: stehlik@fzu.cz. Tel: +420-220 318 475.

Notes

The authors declare no competing financial interest.

ACKNOWLEDGMENTS

This work was supported by the Grant Agency of the Czech Republic (203/08/1445) and from the P108/12G108 (GACR Excellence Center) project. J. Libertinova is acknowledged for SEM images and M. Davydova for lithographic work.

REFERENCES

(1) Tröger, J. *J. Prakt. Chem.* **1887**, *36*, 225−245.
(2) Adrian, J. C., Jr.; Wilcox, C. S. *J. Am. Chem. Soc.* **1989**, *111*, 8055−8057.
(3) Adrian, J. C., Jr.; Wilcox, C. S. *J. Am. Chem. Soc.* **1992**, *114*, 1398−1403.
(4) Goswami, S.; Ghosh, K.; Dasgupta, S. *J. Org. Chem.* **2000**, *65*, 1907−1914.
(5) Claessens, N.; Pierard, F.; Bresson, C.; Moucheron, C.; Mesmaeker, A. K-D. *J. Inorg. Biochem.* **2007**, *101*, 987−996.
(6) Yuan, C. X.; Xin, Q.; Liu, H. J.; Wang, L.; Jiang, M. H.; Tao, X. T. *Sci. China Chem.* **2011**, *54* (4), 587−595.
(7) Dolenský, B.; Elguero, J.; Král, V.; Pardo, C.; Valík, M. *Adv. Heterocycl. Chem.* **2007**, *93*, 1−56.
(8) Sergeyev, S. *Helv. Chim. Acta* **2009**, *92*, 415−444.
(9) Dolenský, B.; Havlík, M.; Král, V. *Chem. Soc. Rev.* **2012**, *41*, 3839−3858.

(10) Wang, Q.; Qu, S. L.; Fu, S. Y.; Liu, W. J.; Li, J. J.; Gu, C. Z. *J. Appl. Phys.* **2007**, *102*, 103714.
(11) Helwig, A.; Muller, G.; Garrido, J. A.; Eickhoff, M. *Sens. Actuators B* **2008**, *133*, 156−165.
(12) Kromka, A.; Davydova, M.; Rezek, B.; Vanecek, M.; Stuchlik, M.; Exnar, P.; Kalbac, M. *Diam. Relat. Mater.* **2010**, *19*, 196−200.
(13) Davydova, M.; Kromka, A.; Rezek, B.; Babchenko, O.; Stuchlik, M.; Hruska, K. *Appl. Surf. Sci.* **2010**, *256*, 5602−5605.
(14) Lee, B. J.; Ahn, B. T.; Lee, J. K.; Baik, Y. J. *Diamond Relat. Mater.* **2001**, *10*, 2174−2177.
(15) Conte, G.; Rossi, M. C.; Salvatori, S.; Tersigni, F.; Ascarelli, P.; Cappelli, E. *Appl. Phys. Lett.* **2003**, *82*, 4459−4461.
(16) Girija, K. G.; Betty, C. A. *Diamond Relat. Mater.* **2004**, *13*, 1812−1815.
(17) Ye, H.; Jackman, R. B.; Hing, P. *J. Appl. Phys.* **2003**, *94*, 7878−7882.
(18) Rezek, B.; Čermák, J.; Kromka, A.; Ledinský, M.; Hubík, P.; Mareš, J. J.; Purkrt, A.; Cimrová, V.; Fejfar, A.; Kočka, J. *Nanoscale Res. Lett.* **2011**, *6*, 238.
(19) Čermák, J.; Rezek, B.; Kromka, A.; Ledinský, M.; Kočka, J. *Diamond Relat. Mater.* **2009**, *18*, 1098−1101.
(20) Havlík, M.; Král, V.; Kaplánek, R.; Dolenský, B. *Org. Lett.* **2008**, *10*, 4767−4769.
(21) Davydova, M.; Stuchlik, M.; Rezek, B.; Kromka, A. *Vacuum* **2012**, *86*, 599−602.
(22) Kromka, A.; Rezek, B.; Remes, Z.; Michalka, M.; Ledinsky, M.; Zemek, J.; Potmesil, J.; Vanecek, M. *Chem. Vap. Deposition* **2008**, *14*, 181−186.
(23) May, P. W. *Philos. Trans. R. Soc. London, Ser. A* **2000**, *358*, 473−495.
(24) Verveniotis, E.; Kromka, A.; Ledinský, M.; Rezek, B. *Diamond Relat. Mater.* **2012**, *24*, 39−43.
(25) Hubík, P.; Mareš, J. J.; Kozak, H.; Kromka, A.; Rezek, B.; Krištofík, J.; Kindl, D. *Diamond Relat. Mater.* **2012**, *24*, 63−68.
(26) Rezek, B.; Krátká, M.; Kromka, A.; Kalbacova, M. *Biosens. Bioelectron.* **2010**, *26*, 1307−1312.
(27) Krátká, M.; Kromka, A.; Ukraintsev, E.; Brož, A.; Kalbacova, M.; Rezek, B. *Sens. Actuators B* **2012**, *166−167*, 239−245.
(28) Maier, F.; Riedel, M.; Mantel, B.; Ristein, J.; Ley, L. *Phys. Rev. Lett.* **2000**, *85*, 3427.
(29) Landstrass, M. I.; Ravi, K. V. *Appl. Phys. Lett.* **1989**, *55*, 1391.
(30) Maki, T.; Shikama, S.; Komori, M.; Sakaguchi, Y.; Sakuta, K.; Kobayashi, T. *Jpn. J. Appl. Phys.* **1992**, *31*, 1446.
(31) Larsson, K.; Ristein, J. *J. Phys. Chem. B* **2005**, *109*, 10304−10311.
(32) Rezek, B.; Ukraintsev, E; Michalíková, A.; Kromka, A; Kalbacova, M. *Sensors* **2009**, *9*, 3549−3562.